Advantages of chromatic-confocal spectral interferometry in comparison to chromatic confocal microscopy

Wolfram Lyda[1,#], Marc Gronle[1], David Fleischle[1,2], Florian Mauch[1] and Wolfgang Osten[1]

1 Institut für Technische Optik, Pfaffenwaldring 9, 70569 Stuttgart
2 Graduate School of Excellence advanced Manufacturing Engineering, Universität Stuttgart, Nobelstr. 12, 70569 Stuttgart
Corresponding Author / E-mail: lyda@ito.uni-stuttgart.de, TEL: +49-(0)711-685-66594 FAX: +49-(0)711-685-66586

KEYWORDS: chromatic confocal sensor, chirp comparison standard, chromatic confocal spectral interferometry, sensor characterization, optical metrology

Chromatic confocal microscopy (CCM) and spectral interferometry (SI) are established and robust sensor principles. CCM is a focus based measurement principle, whose lateral and axial resolution depends on the sensor's numerical aperture (NA), while the measurement range is given by the spectral bandwidth and the chromatic dispersion in axial direction. Although CCM is a robust principle, its accuracy can be reduced by self-focusing effects or asymmetric illumination of the sensor pupil. Interferometric principles based on the evaluation of the optical path difference, e.g. SI, have proven robust against self-focusing. The disadvantage of SI is its measurement range which is limited by the depth of focus. Hence, the usable NA and the lateral resolution are restricted. Chromatic confocal spectral interferometry (CCSI) is a combination of SI and CCM, which overcomes these restrictions. The increase of robustness of CCSI compared to CCM due to the interferometric gain has been demonstrated before. In this contribution the advantages of CCSI in comparison to CCM concerning self-focusing artifacts will be demonstrated. Therefore a new phase evaluation algorithm with higher resolution concerning classical SI-based evaluation algorithms is presented. For the comparison, of the different sensor systems a chirp comparison standard is used.

Manuscript received: January XX, 2011 / Accepted: January XX, 2011

NOMENCLATURE

CCM = chromatic-confocal microscopy

CCSI = chromatic-confocal spectral interferometry

DOE = diffractive optical element

OPD = optical path difference

RMS = root mean square

SI = spectral interferometry

1. Introduction

In recent years an increasing ratio of optical sensors are integrated into coordinate measurement machines for form, layer thickness and topography measurements due to their advantages in terms of contact free and fast measurements. One suitable single shot measurement principle for surface metrology on uncooperative surfaces is the chromatic confocal spectral interferometry (CCSI) [1-3], a hybrid principle combining the robustness and high lateral resolution of chromatic confocal microscopy (CCM) [4] with the advantages of spectral interferometry (SI) [5.7], the interferometric gain and a distance measurement by phase evaluation.

In the standard envelope evaluation used for CCSI and CCM sensors deliver robust measurement results, artifacts can occur on curved mirror like surfaces. In this contribution we present a novel phase evaluation based method for CCSI which is more robust against focusing artifacts.

2. Measurement principle

As mentioned before, CCSI (fig. 1) is a hybrid, single shot measurement principle combining the high lateral resolution and robustness of confocal microscopy with the advantage of spectral interferometry, the heterodyne gain [1, 2, 3]. CCSI is based on chromatic confocal microscopy (CCM) [4], which utilizes a chromatically dispersed object wave to achieve a wavelength

depending focus position in the object space. The backscattered light from the specimen is filtered by a pinhole and, in case of a single shot sensor, sampled with a spectrometer. Due to the confocal filtering, the intensity peak is detected for the wavelength which is focused on the object (fig. 2a).

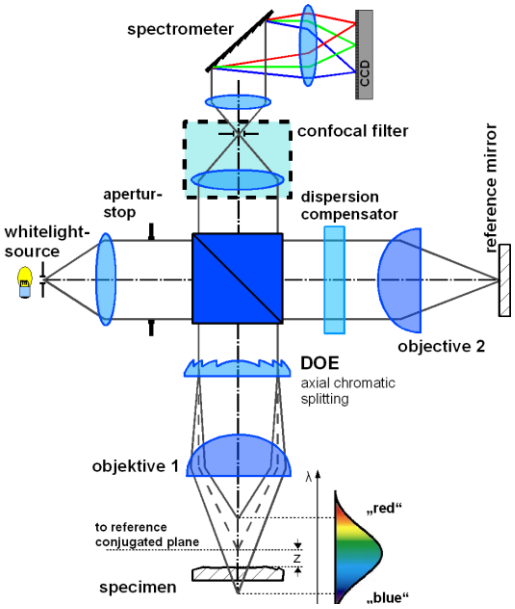

Fig. 1 Basic setup for CCSI in Linnik-architecture

In contrast to the focused based CCM, SI [5-7] is an absolute measurement principle based on the evaluation of the optical path difference (OPD) between the object wave and a reference wave. Changes in the OPD lead to a frequency change of the wavelet in the measurement signal. The evaluation of the OPD leads to a high robustness against self focusing effects in comparison to CCM. The disadvantages of SI are the limitation of the measurement range to the depth of focus leading to a limitation in the system's numerical aperture and the non uniform lateral resolution over the measurement range [10].

CCSI balances the limitations of SI and CCM by combining both principles and their advantages in a single setup (fig. 1). Figure 2 shows the CCM signal and the CCSI-signal. The combination of the dispersed object wave with the reference wave leads to an intensity signal which contains the object height in the wavelet position and the wavelet frequency. The intensity I can be expressed by

$$I(z,d_0,k)=I_O(z)+I_R(k)+2\sqrt{I_O(z)\cdot I_R(k)}\cos(k\cdot(d_0+2z)+\varphi_D(k)) \quad (1)$$

where $\varphi_D=\varphi_O-\varphi_R$ reflects unbalanced dispersion between the interferometer arms, z is the distance of the object to a reference focus, k is the wavenumber and d_0 reflects the OPD between the reference plane and the plane with $z=0$. I_O and I_R are the intensities of the object and the reference wave [1].

3. Signal evaluation for CCSI

Up to now, two different evaluation methods have been used for the signal evaluation [1, 10], the envelope evaluation similar to CCM and the phase evaluation analog to SI. A third method is the calculation of the wavelet phasing analog to a lock-in detection as used in scanning white light interferometry.

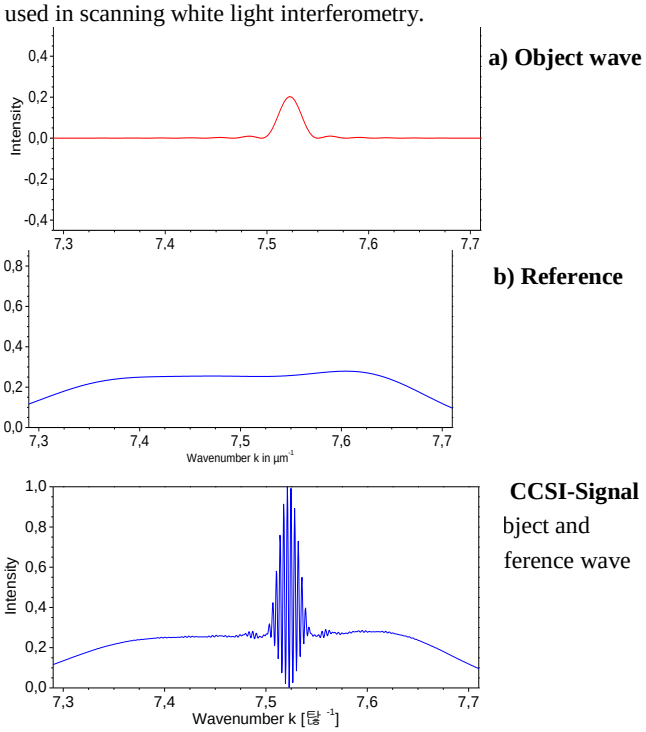

Fig. 2 CCSI-Signal, (a) object signal similar to CCM signal, (b) reference signal and (c) CCSI interference signal

3.1 Envelope evaluation

In Papastathopoulos et. al [1] a signal evaluation algorithm for the separation of signal envelope and the cosine function have been presented. The spectrometer signal is Fourier transformed. The negative part and the zero order of the transformed signal are suppressed and it is transformed back into the frequency domain. The result is a complex function which can be separated into the amplitude

$$A(z,k)=\sqrt{I_O(z,k)\cdot I_R(k)} \quad (2)$$

and the phase. Due to the confocal discrimination of the dispersed object wave the amplitude $A(k,z)$ is a sinc²-distributed intensity over the wavenumber which position depends on the specimen position z analog to CCM [1, 4] (fig 2a, 2c). Using the centre of gravity algorithm, the spectral position can be computed. To obtain the height z from the spectral position, lookup tables or polynomial fits are suitable. With the center of gravity algorithm a resolution around 1% of the full width half maximum of the signal can be obtained [11].

3.2 Absolute phase evaluation

The absolute phase evaluation uses the information stored in the argument of the cosine term of equation (1)

$$\varphi(k)=k(d_0+2z)+\varphi_D(k), \quad (3)$$

In the case of a perfectly balanced interferometer with the same dispersion in the reference and object arm, the phases cancel each other and the optical path difference can be computed by differentiating equation 3 with respect to the wavenumber k.

$$d=\frac{\partial\varphi(k)}{\partial k} \quad (4)$$

Besides the envelope, the complex function computed by the algorithm in section 3.1 contains these phase information, but the

algorithm has proven not robust in comparison to other SI evaluation methods. In Debnath et al. [12] several SI evaluation methods are discussed. One of these methods, the five step spatial phase shifting algorithm, gives robust results and has a fast computation time for single shot CCSI.

The resolution of the phase evaluation is inversely proportional to the bandwidth of the light source [13]. Due to the reduction of the spectrum by the confocal filtering, the depth resolution of CCSI is decreased in comparison to classical SI. Nevertheless a submicron resolution is still obtained [10].

3.3 Phase evaluation by lock-in detection

A new evaluation approach is the calculation of the interference signal phasing as a non absolute measurement value. Therefore a lock-in detection algorithm, for instance described in Fleischer et *al.* [14], will be applied.

The spectrally encoded interference signal of CCSI and SI sensor as a function of the wave number k and the OPD d of the sampled point is generally written as

$$I(d,k) = \alpha(k) + \beta(k)\cos(kd + \varphi). \tag{5}$$

The terms α(k) and β(k) are supposed to be slowly varying functions of k. In order to get the phase information $kd+\varphi$ (equation 5) is firstly multiplied with a chirped, complex carrier signal I_c

$$I_c = \exp(ikd_o), \tag{6}$$

with a constant d_0 which should be close to the real OPD d. The resulting interference signal is split into its real and imaginary part

$$\begin{aligned} I_{\mathrm{Re}}(d,k) &= \frac{1}{2}\left(\alpha(k)\cos(kd_0) + \beta(k)\left(\cos(k\Delta d + \varphi) + \cos(k(d+d_0)+\varphi)\right)\right) \\ I_{\mathrm{Im}}(d,k) &= \frac{1}{2}\left(\alpha(k)\sin(kd_0) - \beta(k)\left(\sin(k\Delta d + \varphi) + \sin(k(d+d_0)+\varphi)\right)\right) \end{aligned} \tag{7}$$

with $\Delta d = d - d_0$. Now these signals are sent through a low-pass filter with zero phase shift in all components, which pass the filter. This can be realized by two infinite impulse response filter stages where the signal being filtered by the first filter is turned vice-versa and then filtered again by the second filter [14]. The cut-off frequency is chosen such that only the terms $\cos(k\Delta d+\varphi)$ and $\sin(k\Delta d+\varphi)$ pass the low-pass filter, since Δd is supposed to be very small with respect to d and $(d+d_0)$. Hence, equations (7) become

$$\begin{aligned} I_{\mathrm{Re}}(d,k) &= \frac{1}{2}\left(\beta(k)\left(\cos(k\Delta d + \varphi)\right)\right) \\ I_{\mathrm{Im}}(d,k) &= -\frac{1}{2}\left(\beta(k)\left(\sin(k\Delta d + \varphi)\right)\right). \end{aligned} \tag{8}$$

The term $\beta(k)$, obtained by the quadratic absolute value of I_{Re} and I_{Im}, represents the confocal peak of the measurement and therefore can be seen as weighting factor for the phase evaluation. The point wise phase term $k\Delta d+\varphi$ is obtained by calculating $-atan(I_{Im}/I_{Re})$ for values where $\beta(k)$ is bigger than a certain threshold value T. In order to determine the weighted phase term, the following fast calculation algorithm can be applied [14]:

$$\tan(k\Delta d + \varphi) = -\frac{\sum_{\beta(k)>T} I_{\mathrm{Im}}(d,k)}{\sum_{\beta(k)>T} I_{\mathrm{Re}}(d,k)} \tag{9}$$

The result of the evaluation algorithm is the phase difference to the carrier frequency function (eq. 6) modulated by 2π. To retrieve an absolute measurement value an unwrapping of sequentially measured data or a combination of the different evaluation strategies is necessary.

3.4 Comparison of the evaluation methods

For the comparison of the different evaluation methods a plane mirror was moved in z direction with a piezo stage and the distances were computed with the different evaluation methods. The used CCSI-sensor head is described in chapter 4. Figure 3 shows the predefined movement profile (step width 0.11 µm) and the results from the three algorithms. The center of gravity algorithm shows a high repeatability (RMS of 10 measurements under 10 nm) (fig. 3b). The absolute phase measurement is overlaid with an evaluation noise in the range of the 0.11 µm step height (fig 3c).

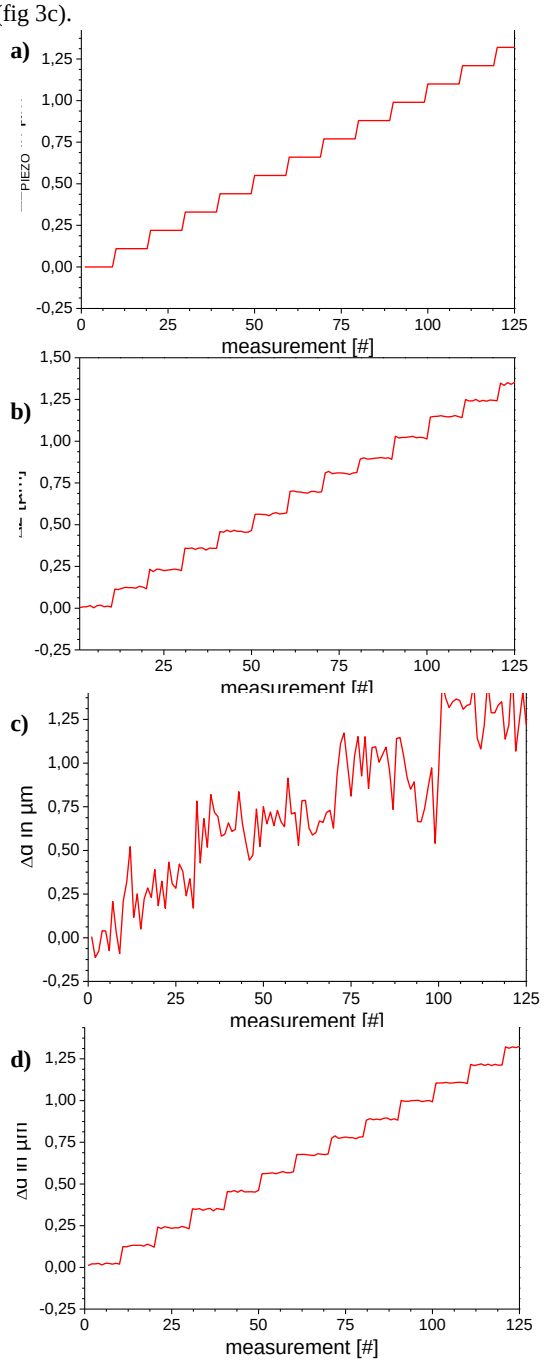

Fig. 3 (a) step profile of the piezo stage, (b) envelope evaluation, (c) absolute phase evaluation, (d) unwrapped lock-in detection

The lock-in detection shows significantly less noise than the absolute phase evaluation (fig. 3d) (RMS of 10 measurements under 10 nm). Due to the step height under the half wavelength an unwrapping between the different piezo steps is possible. Further more the step height is reconstructed with a systematic error of -3%. Due to simulation results this error is assumed to be caused by uncompensated dispersion between the two interferometer arms and a not perfect filter stage in the lock-in algorithm.

4. Sensor hardware

For the comparison of chromatic confocal spectral interferometry and chromatic confocal microscopy different sensor setups are used. The first one is a fiber interferometer with a chromatically dispersed object arm. The splitting of the beams in object and reference arm is realized by a x-coupler. The confocal discrimination is realized with the single mode fiber introduced in [1]. For the illumination, a fiber coupled super luminescence diode (SLD) is used. The spectrally sampled signal is acquired with a fiber coupled spectrometer. The sensor architecture enables a direct comparison of CCM and CCSI with a single sensor setup. Unfortunately the optical path difference between reference arm and object arm is not stable enough for a high accuracy phase evaluation.

To overcome the instable phase problem a more stable sensor based on a Mirau lens architecture was developed (figure 4). The chromatic axial separation of foci and the optical path difference is realized with a DOE placed in the object space. The phase function of the DOE is adapted to the numerical aperture of the Mirau lens and the thickness of the DOE substrate to reduce spherical aberrations introduced by the substrate.

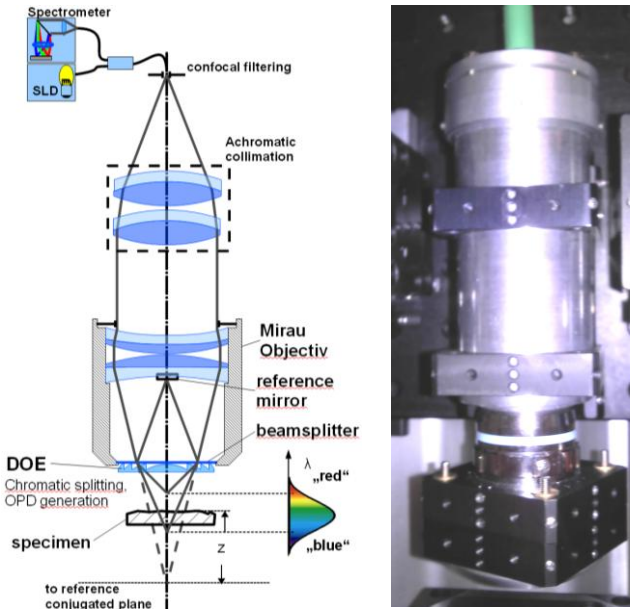

a) b)

Fig. 4 (a) scheme of Mirau based CCSI sensor and (b) picture of sensor head

For this comparison the chromatic confocal sensors (figure 5) use the same light source, fiber coupler and spectrometer. The chromatic axial shift of the foci is introduced by a DOE used as the collimation lens for the fiber output. For a diffraction limited spot in the object plane commercial objective lenses with numerical apertures between 0.5 and 0.95 are available. For the experimental comparison of CCM and CCSI two Olympus front lenses (50x 0.5 and 50x 0.8) were used. The numerical aperture of the second lens is reduced by a limited illumination of the lens pupil to approximately 0.6 enabling a comparison to the CCSI sensor NA.

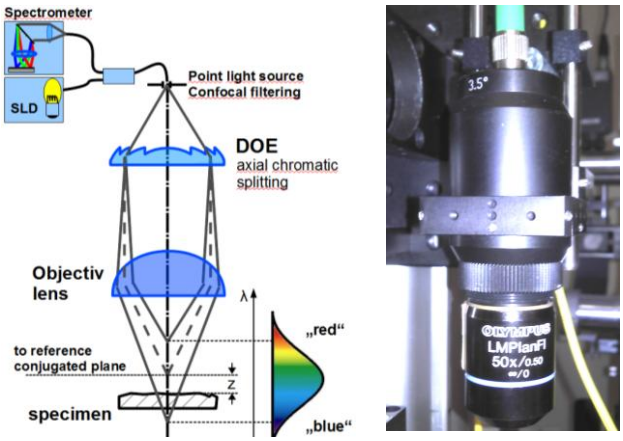

a) b)

Fig. 5: (a) scheme of CCM sensor and (b) picture of sensor head

The parameters of the light source, the spectrometer and the different sensor heads are described in table 1.

Parameter	CCM 1	CCM 2	CCSI-mirau
Light source	SLD λ = 830 nm, Δλ = 50 nm, 16 mW		
Detector	Spectrometer, Δλ < 0.08 nm, 14-bit		
Numerical aperture	0.5	ca 0.62	ca 0.6
Working distance	10 mm	0.6 mm	2 mm
Measurement range	35 µm	35 µm	27µm
Spot size resolution	ca 2 µm	ca 2 µm	2 µm

Tab 1: Properties of CCSI-Sensors

The sensor heads are mounted on a 3-axis state with a certified accuracy and flatness smaller than 1µm. For fast z-scans an additional piezo stage is mounted on the stage to move the specimen with nanometer resolution.

5. Experimental comparison

As mentioned before CCSI has two advantages in comparison to CCM. Namely the interferometric gain and the additional phase information. In former publications [8, 9] the raise of robustness due to interferometric gain on uncooperative specimens like edge regions on blazed gratings and DOEs was described. This contribution concentrates on the reduction of self focusing effects on curved optical surfaces by an additional phase evaluation. For this comparison, we use the so called chirp comparison standard developed by the PTB, Germany [15] (figure 6). The contour of the chirp comparison standard consists of a symmetrically arranged cosine profile with decreasing periods between 91 µm and 10 µm. The profile has an amplitude of approximately 0.45 µm.

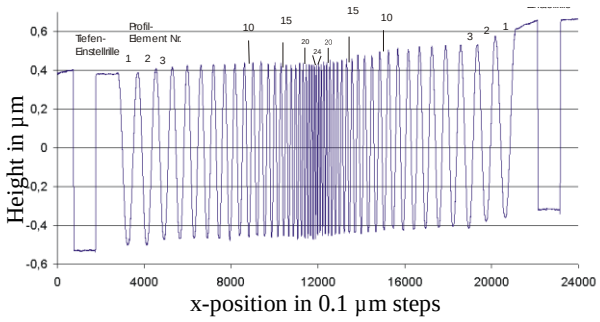

Fig. 6: Exemplary measurement of chirp comparison standard prototype developed by PTB [15] (source: data sheet)

In figure 7 the measurement results of the chirp comparison standard with chromatic confocal microscopy are shown.

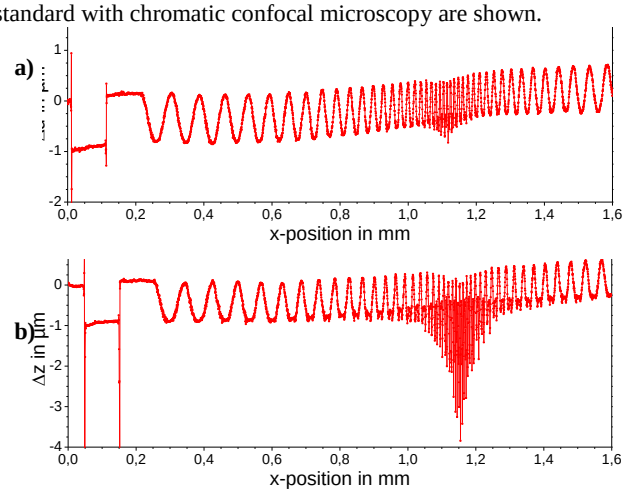

Fig. 7: Measurement of the chirp comparison standard with CCM 0.5 µm step width, envelope evaluation with center of gravity of full width half maximum, (a) 50x NA 0.62 objective lens and (b) 50x NA 0.5

The measurements show artifacts on the extreme points of the cosine profile. Figure 8 shows two higher resolved slices of the chirp comparison standard. In the region of the lower extreme point of the cosine profile the artifacts cause inverse curvatures.

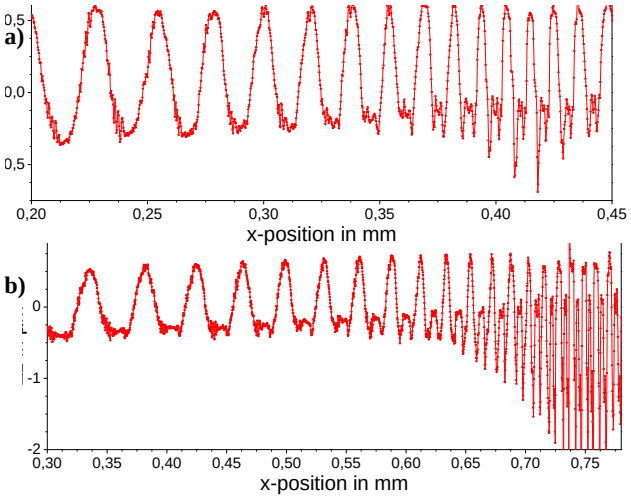

Fig. 8 Measurement of the center of the chirp comparison standard with CCM 0.2 µm step width, (a) 50x NA 0.62 and (b) 50x NA 0.5

Such artifacts are usually caused by self focusing effects, which deform the signal envelope and move the signal's center of gravity. The artifacts in the middle of the chirp are caused by a combination of self-focusing and limited resolution. Both artifact types depend on the numerical aperture of the objective lenses (figure 8a vs. b). The measurements taken with CCSI show similar artifacts caused by resolution problems in the envelope evaluation results.

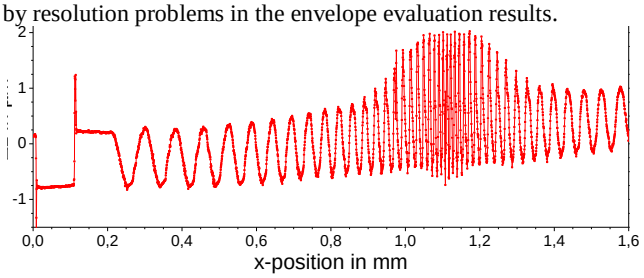

Fig. 9 Measurement of the chirp comparison standard with CCSI, 0.5 µm step width, envelope evaluation with center of gravity of full width half maximum

As mentioned before the absolute phase measurement is not suitable due to the bandwidth dependent axial resolution limits. Hence the lock-in detection algorithm is used to estimate the phase difference between two measurements. In the figures 10 and 11 the unwrapped phase results of the chirp measurement are shown. The artifacts from the envelop evaluation do not appear in the phase evaluation results.

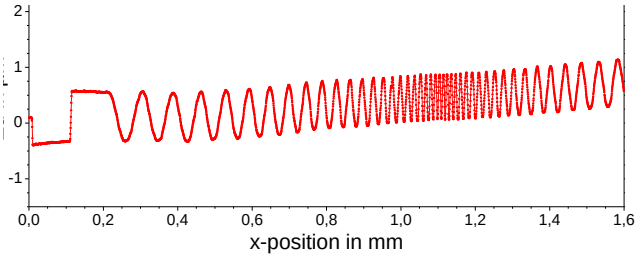

Fig. 10 Measurement of the chirp comparison standard with CCSI, 0.5 µm step width, lock-in evaluation after unwrapping

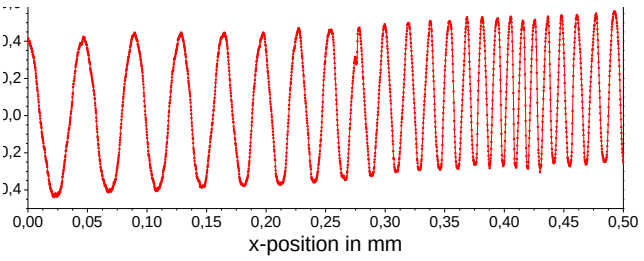

Fig. 11 Measurement of the chirp comparison standard with CCSI, 0.5 µm step width, lock-in evaluation after unwrapping

For the validation of the results of the lock-in detection the periods of the cosines are extracted from the measurement results of figure 10 and are compared to the periods from the calibration sheet. The comparison is shown in figure 12.

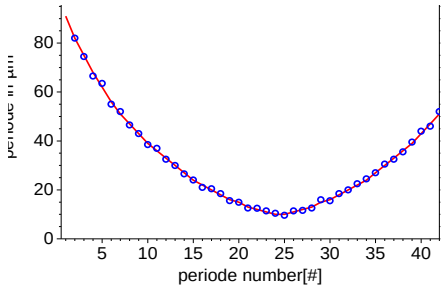

Fig. 12 Evaluated periods from the measurement shown in figure 10 (circles) and the periods from the data sheet of the chirp calibration standard (line)

A good agreement between measurement and data sheet is achieved. For further characterizations regarding the linearity and correlation with the cosine profile a calibration of the chirp comparison standard is needed which is not available at the moment.

6. Conclusion

In this contribution we presented a new evaluation method for CCSI which increases the resolution of phase evaluation. With this evaluation method the robustness of CCSI measurements on curved surfaces is increased. The new phase evaluation compensates the influence of self-focusing effects. The measurement results on the chirp comparison standard show its advantages in comparison to classical envelope evaluation of CCSI and CCM-sensors with a similar numerical aperture.

Future research has to deal with strategies for combination of envelope evaluation and look-in detection to achieve a robust and absolute signal evaluation without lateral unwrapping. Furthermore the dispersion correction and the correction of systematic errors are necessary.

ACKNOWLEDGEMENT

We thank the “Deutsche Forschungsgesellschaft” (DFG project OS 111/21-2) and the graduate school of excellence advanced manufacturing engineering (GSAME) for the financial support of this work.

REFERENCES

1. Papastathopoulos, E., Körner, K., Osten, W., “Chromatic Confocal Spectral Interferometry With Wavelet Analysis”, SPIE 6189, 618913 (2006)
2. Papastathopoulos, E., Körner, K., Osten, W., „Chromatic Dispersed Interferometry with Wavelet Analysis”, Opt. Lett. 31, 5, p. 589ff (2006)
3. Papastathopoulos, E., Körner, K., Osten, W., “Chromatic Confocal Spectral Interferometry”, App. Opt. 45, 32, pp 8244ff (2006)
4. Molesini, G., Peidrini, G., Poggi, P., Quercioli, F., “Focus wavelength encoded optical profilometer”, Optics Communications, Vol. 49, Nr. 4, pp. 229ff (1984)
5. Schwider, J., Zhou, L., “Dispersive Interferometric Profilometer”, Opt. Lett. 19, 995-997 (1994)
6. Schnell, U., Zimmermenn, E., Dändliker, R., “Absolute distance measurement with synchronously sampled white-light channeled spectrum”, Pure Appl. Opt. 4, pp. 643-651 (1995)
7. Wojtkowski, M., Leitgeb, R., Kowalczyk, A., Bajraszewski, T., Fercher, A. F., “In vivo human retinal imaging by Fourier domain optical coherence tomography”, J. Biomed. Opt. 7, 457-463 (2002)
8. Papastathopoulos, E., Lyda, W., Körner, K. Osten, W. “Chromatic-confocal spectral-interferometry”, VDI-proceddings 2007, (2007)
9. Lyda, W., Körner, K., Osten, W. “Einsatz der chromatisch-konfokalen spektralen Interferometrie (CCSI) zur Reduktion der Messunsicherheit bei chromatisch-konfokalen Topografiemessungen”, DGaO-Proceedings 2008, ISSN: 1614-8436 (2008)
10. Lyda, W., Ramos de Carvalho, C., Fleischle, D., Mauch, F., Haist, T., Osten, W., “Vor- und Nachteile der chromatisch-konfokalen Spektralinterferometrie im Vergleich zur klassischen Spektralinterferometrie”, DGaO-Proceedings 2010, ISSN: 1614-8436 (20108)
11. Ruprecht A., Wiesendanger, T., Tiziani, H., "Signal evaluation for high-speed confocal measurements", app. opt., vol. 41, 35, pp 7410-7415 (2002)
12. Debnath, S. K., Kothiyal, M. P., Kim S. W., “Evaluation of spectral phase in spectrally resolved white-light interferometry: Comparative study of single-frames techniques“ in Optics and Lasers in Engineering 47, 11, 1125–1130 (2009)
13. Wojtkowski, M., “High-speed optical coherence tomography: basics and applications”, applied optics vol. 49, 16, pp. D30-D61 (2010)
14. Fleischer, M., Windecker, R., Tiziani, H.-J., “ Fast algorithms for data reduction in modern optical three-dimentional profile measurement systems with MMX technology” app. opt. vol. 39, 8, pp 1290-1297 (2000)
15. Krüger-Sehm, R., Bakucz, P., Jung, L., Wilhelms, H.,” Chirp Calibration Standards for Surface Measuring Instruments”, Technisches Messen vol. 74, 11, pp. 572-576 (2007)
16. Lyda, W., Fleischle, D., Haist, T., Osten, W., “Chromatic confocal spectral interferometry for technical surface characterization”, Proc. SPIE 7432, (2010)
17. Fleischle, D., Lyda, W., Mauch, F., Osten, W., “Optical metrology for process control: modeling and simulation of sensors for a comparison of different measurement principles” Proc. SPIE 7718 (2010), S. 77181D-12